

References and Notes

1. H. K. Mao, Y. Wu, L. C. Chen, J. Shu, A. P. Jephcoat, *J. Geophys. Res.* **95**, 21737 (1990).
2. A. K. Singh, H. K. Mao, J. Shu, R. J. Hemley, *Phys. Rev. Lett.* **80**, 2157 (1998).
3. H. K. Mao et al., *Nature* **396**, 741 (1998); *Nature* **399** (correction), 280 (1999).
4. L. Stixrude, R. E. Cohen, *Science* **267**, 1972 (1995).
5. P. Söderlind, J. A. Moriarty, J. M. Wills, *Phys. Rev. B* **53**, 14063 (1996).
6. G. Steinle-Neumann, L. Stixrude, R. E. Cohen, *Phys. Rev. B* **60**, 791 (1999).
7. A. Laio, S. Bernard, G. L. Chiarotti, S. Scandolo, E. Tosatti, *Science* **287**, 1027 (2000).
8. R. Lübbbers, H. F. Grünsteudel, A. I. Chumakov, G. Wortmann, *Science* **287**, 1250 (2000).
9. H. K. Mao et al., personal communication.
10. S. Merkel, A. F. Goncharov, H. Mao, P. Gillet, R. J. Hemley, *Science* **288**, 1626 (2000).
11. E. Burkel, *Inelastic Scattering of X-rays with Very High Energy Resolution* (Springer, New York, 1991).

12. G. Ruocco et al., *Nature* **379**, 521 (1996); M. Krisch et al., *Phys. Rev. B* **56**, 8691 (1997).
13. H. K. Mao, P. M. Bell, J. W. Shaner, D. J. Steinberg, *J. Appl. Phys.* **49**, 3276 (1978).
14. Angle-dispersive XRD experiments were carried out at the ID30 high-pressure beamline at a wavelength of 0.3738 Å. Patterns were collected on imaging plates located 350 mm from the sample. The x-ray beam size at the sample location was 10 μm by 15 μm.
15. N. Von Bargen, R. Boehler, *High Pressure Res.* **6**, 133 (1990).
16. V. J. Minkiewicz, G. Shirane, R. Nathans, *Phys. Rev.* **162**, 528 (1967).
17. J. L. Warren, J. L. Yarnell, G. Dolling, R. A. Cowley, *Phys. Rev.* **158**, 805 (1967).
18. M. W. Guinan, D. N. Beshers, *J. Phys. Chem. Solids* **29**, 541 (1968).
19. Web fig. 1 is available at www.sciencemag.org/cgi/content/full/291/5503/468/DC1/.

20. J. M. Brown, R. G. McQueen, *J. Geophys. Res.* **91**, 7485 (1986).
21. F. Birch, in *Solids Under Pressure*, W. Paul, D. M. Warschauer, Eds. (McGraw-Hill, New York, 1963), pp. 137–162; *Geophys. J. R. Astron. Soc.* **4**, 295 (1961).
22. A. M. Dziewonski, D. L. Anderson, *Phys. Earth Planet. Inter.* **25**, 297 (1981).
23. A. P. Jephcoat, P. Olson, *Nature* **325**, 332 (1987).
24. H. R. Wenk, S. Matthies, R. J. Hemley, H. K. Mao, J. Shu, *Nature* **405**, 1044 (2000).
25. We thank S. Merkel, H. R. Wenk, and H. K. Mao for communicating unpublished results and B. Couzinet and J. C. Chervin for their help in the preparation of the samples and high-pressure cells. M. Mezouar is warmly acknowledged for his help during the unscheduled XRD experiments carried out at the ID30 beam station (at ESRF). Contribution CNRS-INSU IT 257.

27 September 2000; accepted 7 December 2000

The Role of Br₂ and BrCl in Surface Ozone Destruction at Polar Sunrise

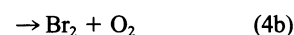
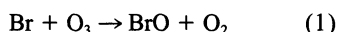
Krishna L. Foster,¹ Robert A. Plastridge,² Jan W. Bottenheim,³ Paul B. Shepson,⁴ Barbara J. Finlayson-Pitts,¹ Chester W. Spicer^{2*}

Bromine atoms are believed to play a central role in the depletion of surface-level ozone in the Arctic at polar sunrise. Br₂, BrCl, and HOBr have been hypothesized as bromine atom precursors, and there is evidence for chlorine atom precursors as well, but these species have not been measured directly. We report here measurements of Br₂, BrCl, and Cl₂ made using atmospheric pressure chemical ionization–mass spectrometry at Alert, Nunavut, Canada. In addition to Br₂ at mixing ratios up to ~25 parts per trillion, BrCl was found at levels as high as ~35 parts per trillion. Molecular chlorine was not observed, implying that BrCl is the dominant source of chlorine atoms during polar sunrise, consistent with recent modeling studies. Similar formation of bromine compounds and tropospheric ozone destruction may also occur at mid-latitudes but may not be as apparent owing to more efficient mixing in the boundary layer.

Surface-level O₃ depletion events, at times marked by O₃ mixing ratios below 1 part per billion (ppb) (nmol/mol air), have been observed at polar sunrise (March through May) throughout the Arctic for over a decade (1–4). This depletion has been shown to be correlated with Br associated with particles (3, 5), leading to the hypothesis that the O₃ depletion is caused by a chain reaction initiated by a Br atom (3). Laboratory kinetic experiments and mechanistic data suggest that the chain is initiated through the photolysis of gas phase Br

compounds (6–8). The BrO free radical, a key intermediate in the Br-catalyzed destruction of O₃, has been observed at ground level over the Arctic (9, 10). Although the source of active Br is believed to be oxidation of Br⁻ in sea-salt aerosol, snow, and frozen ocean surfaces (11, 12), the mechanism is not well understood. The key to elucidating the chemistry leading to lower atmospheric ozone depletion in the Arctic, and possibly at mid-latitudes, is the measurement of specific gaseous halogen compounds present before and during ozone depletion episodes.

Ozone depletion by gas phase Br reactions occurs via reactions 1 to 5:

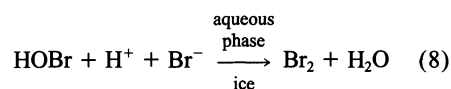


Cross-reactions of BrO with ClO may also be important (13):



Removal of Br atoms from the chain occurs through reactions with organic compounds such as formaldehyde, which are present in measurable concentrations in the polar spring at high Arctic sites (14). The Br⁻ ion in the product HBr is then temporarily sequestered in aerosol, surface snow, and ice.

To sustain the chain destruction of ozone, there must be heterogeneous reactions to activate Br⁻ ions from aerosol and surface snowpack into a gaseous photochemically active form. For example, the uptake of gaseous HOBr on snow followed by its reaction with Br⁻ was suggested as a recycling mechanism for Br₂ in the Arctic (15):



There is laboratory evidence for the production of Br₂ via reaction 8 [e.g., (16, 17)].

Previous measurements indicated the presence of a large source of photochemically active Br and Cl precursors (6, 7), but the technique used was nonspecific and therefore left proof for the presence of Br₂ and other halogen atom precursors open. Here we report results from specific measurements of Br₂, BrCl, and Cl₂ in the troposphere of the high Arctic, ~125 cm above the snow.

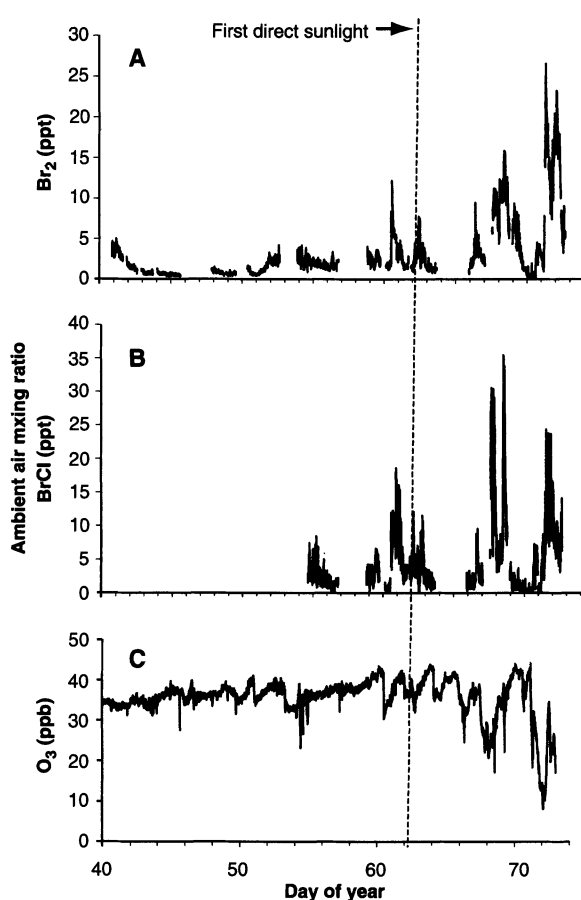
Figure 1 shows the mixing ratios of Br₂, BrCl, and O₃ between 9 February and 13 March 2000 (day of year 40 to 73) (18). BrCl was first observed above the 2-ppt detection limit on day 54 (23 February). The maximum Br₂ and BrCl

¹Department of Chemistry, University of California, Irvine, CA 92697–2025, USA. ²Battelle, 505 King Avenue, Columbus, OH 43201–2693, USA. ³Environment Canada, 4905 Dufferin Street, Toronto, Ontario M3H 5T4, USA. ⁴Department of Chemistry and Department of Earth and Atmospheric Sciences, Purdue University, West Lafayette, IN 47907–1393, USA.

*To whom correspondence should be addressed. E-mail: spicerc@battelle.org

REPORTS

Fig. 1. Ambient mixing ratios of (A) Br₂ with the ion pair 158/79. The same mixing ratios of Br₂ are derived with the 160/79 or 160/81 ion pairs. (B) BrCl with the ion pair 114/35. The same mixing ratios of BrCl are derived with the 116/35 and 116/37 ion pairs. (C) O₃ between days 40 and 73 (9 February to 13 March). The blank areas are periods where field calibrations and zeroes were performed or other species were being monitored. Signals were observed for the ion pairs associated with BrCl starting on day 50, but were not above the statistical detection limit until day 54.

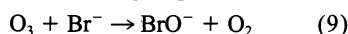


mixing ratios were 27 ppt Br₂ on day 71 and 35 ppt BrCl on day 68. Trends in BrCl and Br₂ are similar, suggesting a common source. Cl₂ was never observed above the detection limit of 2 ppt. Figure 1C shows the measured O₃ mixing ratios, which were typically 30 to 40 ppb during the initial dark period, as expected for relatively clean background air (19), and as found previously at Alert before sunrise. Variations in Br₂, BrCl, and O₃ result from changes in meteorology (wind direction, height of the inversion layer, and stability of the air parcel) and in the chemistry producing the halogens (6, 7, 9).

Several ozone depletion episodes occurred, one on days 67 to 69 when O₃ dropped from ~40 to 22 ppb, and one on days 71 to 72 when O₃ dropped to 11 ppb. Br₂ and BrCl both decreased as the ozone recovered. Similar behavior was seen on days 60 and 66, where smaller O₃ depletion events occurred. These negative correlations between Br₂/BrCl and O₃ are consistent with the negative correlation between photolyzable gaseous halogen compounds and O₃ reported by Impey and co-workers (6, 7), as well as that between “filterable Br” and O₃ first reported at Alert (3) and later at Spitsbergen, Svalbard (4). The levels of O₃ and the Br compounds in air after sunrise at Alert will be influenced by air-mass history. Near surface air-mass back trajectories (925 mbar isobaric) for the period 10 to 12 March (days 70 to 72) indicate surface-level air arriving from the northeast over

the Arctic Ocean, north of Greenland. In contrast, back trajectories for the period 26 to 28 February (days 57 to 59) indicate local air-mass origin from the east, off Greenland via the Nares Strait. Trajectories from either Ellesmere to the south or Greenland to the east tend to cause mixing of free tropospheric ozone into the boundary layer air, and higher ozone mixing ratios, near 40 ppb (20). At 210 m above sea level, the site at Alert is often above the Arctic Ocean boundary layer, and during these periods will not be exposed to Br species emitted at the ocean surface, nor to the O₃ depletions that may result from their photolysis.

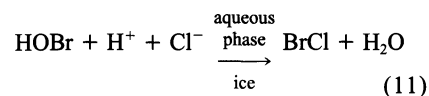
The monitoring period began in complete darkness. As a result, Br activation mechanisms that require sunlight, such as the oxidation of Br⁻ by OH (21), are not applicable under these conditions. Direct sunlight was not present at Alert before 2 March (day 62), and even then, only for a few minutes each day (22). Laboratory experiments suggest that a possible mechanism for production of Br₂ in the dark is the oxidation of Br⁻ in Br⁻-laden ice or snow by O₃ (23), by the following proposed mechanism:



The HOBr then undergoes reaction 8 with Br⁻ to generate Br₂.

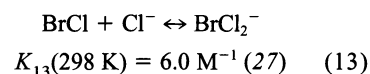
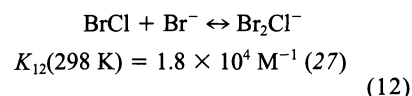
Furthermore, BrCl is anticipated as a precursor in the ozone destruction cycle from

reaction 11 of HOBr with Cl⁻, which has been probed in laboratory (17, 24) and modeling studies of mid-latitude and Arctic chemistry (25, 26):

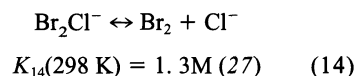


The kinetics of reactions 8 and 11 on ice surfaces at lower temperatures and in solution at room temperature (27) are similar, so that the loss process for HOBr formed by reaction 9 followed by reaction 10 will depend on the relative amounts of Cl⁻ and Br⁻ ions available for reaction. In seawater, the molar ratio of Cl⁻ to Br⁻ is 650:1 (19). However, studies of phase transitions in seawater by Molina and co-workers (28) suggest that Cl⁻ will be concentrated by a factor of ~11 and Br⁻ by a factor of ~38 in seawater deposited on the ice pack under conditions of polar sunrise. This would decrease the Cl⁻/Br⁻ ratio to 188. Further support for enhancement of Br⁻ is found in the observation of preferential surface segregation of Br⁻ in NaCl crystals doped with small amounts of Br⁻ on exposure to water vapor (29). In addition, recent studies of the reactions of deliquesced NaCl aerosol have shown the ready availability of Cl⁻ ions at the interface (30), attributed to both the size and polarizability of the Cl⁻ anion, and an even greater effect is anticipated for the larger and more polarizable Br⁻ ion; hence, if the reaction occurs at the interface, Br chemistry may be enhanced. At Alert in the February to March time frame, the Cl⁻/Br⁻ ratio in fresh snowfall ranges from ~50 to 200 (31), and enhanced mixing ratios of Br⁻ relative to Cl⁻ were measured in the snowpack during this study (32).

The measured ratio of BrCl to Br₂ in the air is ~1, rather than ~50 to 650, which might be expected on the basis of the relative amounts of Cl⁻ and Br⁻ in salt on the snowpack and in seawater. The Henry's Law constant for BrCl at 245 K is calculated to be 60 M atm⁻¹ on the basis of recent measurements (33), compared with 13 M atm⁻¹ for Br₂. This decreased solubility of Br₂ compared with BrCl should enhance the gas phase Br₂ mixing ratios relative to BrCl. Furthermore, the increased solubility of BrCl will increase the opportunities for it to undergo secondary reactions in the surface film (27):

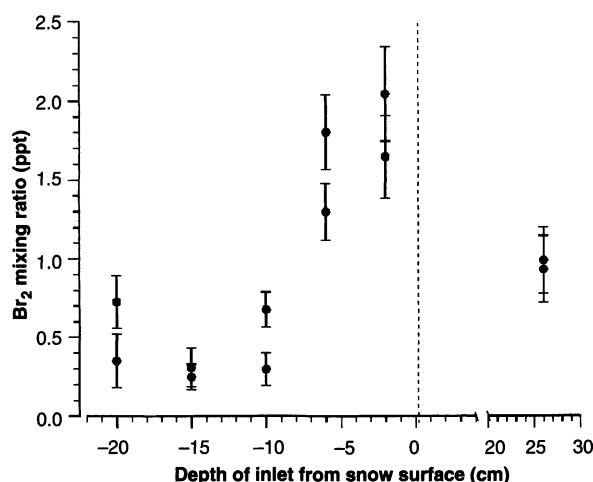


The Br₂Cl⁻ formed in reaction 12 decomposes to Br₂ and Cl⁻:



REPORTS

Fig. 2. Br₂ mixing ratios measured with the ion pair 158/79 in snowpack interstitial air and in the air above on day 63 (3 March). Error bars are $\pm 2\sigma$.



Sea-salt particles in the snowpack in the Arctic are likely to be liquid (28), so that similar reactions of BrCl might be anticipated at the snowpack surface. At room temperature, the equilibrium constant K_{12} is larger than K_{13} by a factor of 3000. If this is also the case at the lower temperatures (~ 240 K) characteristic of the Arctic at this time of year, it more than overcomes the smaller concentrations of Br⁻ in seawater, which would otherwise favor reaction 13. In short, the observation that gaseous BrCl and Br₂ are typically present at similar mixing ratios suggests that most of the BrCl undergoes secondary reactions in the ice surface layer to form Br₂, in competition with release to the gas phase. A detailed multiphase modeling study (26) updated with more recent rate constants for the reaction of BrO with aldehydes (34) indicates a BrCl/Br₂ ratio at peak concentrations ranging from 0.7 to 1.4, consistent with our measurements.

The observed simultaneous increases of Br₂ and BrCl mixing ratios during ozone depletion episodes is likely due to photolysis of Br₂ and BrCl causing O₃ depletion and HOBr formation by reactions 1 and 2. Subsequent heterogeneous reactions 8 and 11 of HOBr with Br⁻ and Cl⁻ on the snowpack produce more Br₂ and BrCl, leading to increases in their mixing ratios. The decrease in Br₂ and BrCl as O₃ recovers is likely due to mixing with free tropospheric air, or to a change in air mass to one that experienced less time over the Arctic Ocean surface, which is known to have a higher halide ion content.

The relative importance of BrCl and Br₂ as Br atom precursors can be calculated from the product $(J_7/2J_3) \cdot ([BrCl]/[Br_2])$; for the peak mixing ratios measured on day 71, we obtain 0.15 using the relative J values estimated by Michalowski *et al.* (26). Thus, it appears that at the time of sunrise, Br₂ photolysis is likely to be the dominant source of Br atoms.

That heterogeneous reactions on the snowpack such as reaction 8 are involved in the production of Br₂ was confirmed by measuring

the Br₂ mixing ratio in the snowpack interstitial air with an all-Teflon snow probe, as well as in the air above the snowpack surface. The mixing ratios of Br₂ in interstitial air just below the air-snow interface were about twice those measured minutes later above the surface (Fig. 2). The depth profile of Br₂ in the snowpack is consistent with the observation of higher Br⁻ concentrations in the surface snow than at deeper levels. Bromide ions were measured in the surface snow in February at this site at an average concentration of 3.5×10^{-7} M, but decreased by more than an order of magnitude in lower layers. There was also a strong vertical gradient in O₃ in the snowpack air; O₃ typically decreased by 50% over the first 10 cm of snow.

Although these observations were made in the polar boundary layer, similar chemistry is anticipated in mid-latitudes (25) where, however, lower mixing ratios of Br₂ and BrCl are expected owing to more rapid mixing of boundary layer air masses with the free troposphere, and to more rapid photolysis of the halogens. During studies of Cl₂ on the coast of Long Island, New York (35), there was a small signal of the ion pairs used to monitor Br₂; however, because the signals did not exceed the calculated detection limit of 6 ppt, they were not reported. Nevertheless, those observations, combined with the findings presented here, suggest that Br may be an important contributor to O₃ loss in the lower atmosphere globally. This is consistent with recent reports of ozone variability over the Indian Ocean, which were best explained by a contribution from Br chemistry (36), and with some ozone destruction in the subtropical Northwestern Pacific Ocean just after sunrise, which appears to be associated with halogens in sea-salt particles.

References and Notes

1. J. W. Bottenheim, A. G. Gallant, K. A. Brice, *Geophys. Res. Lett.* **13**, 113 (1986).
2. S. J. Oltmans, W. D. Komhyr, *J. Geophys. Res.* **91**, 5229 (1986).
3. L. A. Barrie, J. W. Bottenheim, R. C. Schnell, P. J. Crutzen, R. A. Rasmussen, *Nature* **334**, 138 (1988).

4. S. Solberg, N. Schmidbauer, A. Semb, F. Stordal, Ø. Hov, *J. Atmos. Chem.* **23**, 301 (1996).
5. E. Lehrer, D. Wagenbach, U. Platt, *Tellus* **49B**, 486 (1997).
6. G. A. Impey, P. B. Shepson, D. R. Hastie, L. A. Barrie, K. G. Anlauf, *J. Geophys. Res.* **102**, 16005 (1997).
7. G. A. Impey *et al.*, *J. Atmos. Chem.* **34**, 21 (1999).
8. L. Barrie, U. Platt, *Tellus* **49B**, 450 (1997).
9. M. Hausmann, U. Platt, *J. Geophys. Res.* **99**, 25399 (1994).
10. M. Tuckermann *et al.*, *Tellus* **49B**, 533 (1997).
11. D. K. Perovich, J. A. Richter-Menge, *J. Geophys. Res.* **99**, 16341 (1994).
12. S. Martin, Y. Yu, R. Drucker, *J. Geophys. Res.* **101**, 12111 (1996).
13. G. LeBras, U. Platt, *Geophys. Res. Lett.* **22**, 599 (1995).
14. A. L. Sumner, P. B. Shepson, *Nature* **398**, 230 (1999).
15. J. C. McConnell *et al.*, *Nature* **355**, 150 (1992).
16. M. Eigen, K. Kustin, *J. Am. Chem. Soc.* **84**, 1355 (1962).
17. S. Fickert, J. W. Adams, J. N. Crowley, *J. Geophys. Res.* **104**, 23719 (1999).
18. Measurements were made with an atmospheric pressure chemical ionization-tandem mass spectrometer (APCI-MS/MS, PerkinElmer Sciex Model 365) modified for air monitoring (35, 37). A corona discharge was used to ionize the sample air. All measurements were made in the negative-ion mode. For each target chemical, a parent molecular anion was separated from other ions by using the first quadrupole, and then fragmented in a gas collision cell. One or more particular fragments were isolated by the second quadrupole, giving parent-daughter ion pairs that are characteristic of each target chemical. Molecular Br₂ was measured as the ion pairs 158/79, 160/79, 160/81, and 162/81; Cl₂ as 70/35, 72/35, 72/37, and 74/37; and BrCl as 114/35, 116/35, 116/37, and 118/37. Detection limits are estimated to be 0.2 ppt for Br₂ and 2 ppt for Cl₂ and BrCl, respectively, for a 20-s integration time and a signal to noise ratio of 3. The identification of these compounds was confirmed by daughter ion scans of selected parent ions, and measurement of the ratios of observed signals compared with those expected on the basis of the natural abundance of the isotopes found in each compound. Throughout the study, at least two ion pairs were monitored for each compound. The instrument was located in the far transmitter building (FTX; 82°27.29'N, 62°29.84'W) ~ 6 km from the Alert base camp, ~ 7 km south of the Arctic Ocean, and ~ 210 m above sea level. The sample line was an insulated 0.64-cm outer diameter Teflon tube heated to 21°C and extended ~ 7.6 m away from the west wall of the building. Residence time in the sample line was less than 1 s. The data have been corrected for sample line loss measured as 10% for Cl₂ and 4% for Br₂. The inlet was shielded to prevent snow from entering the sampling line. A Teflon solenoid valve, programmed to open and close automatically, was used to record 30-min baseline measurements every 4 to 6 hours by diverting the ambient air flow through a potassium carbonate (K₂CO₃) denuder placed in the air-stream before the mass spectrometer inlet. The denuder removes gaseous halogen compounds from the air stream. Calibrations were performed with Br₂ and Cl₂ permeation devices with permeation rates of 6.3 and 35.7 ng min⁻¹, respectively, which gives calibration concentrations of 111 ppt Br₂ and 1420 ppt Cl₂ in air. The precision of calibration data sets carried out before and after a given ambient air measurement was $\pm 10\%$ (2σ) for all halogens. The permeation rates were checked at the beginning of the study by bubbling the air-stream into a 30 mM NaHCO₃ solution and measuring the Br⁻ and Cl⁻ concentration by ion chromatography. The calibration for BrCl was assumed to be the same as for Cl₂ on the basis of laboratory studies with a similar API-MS (Model 300) in which the sensitivities for BrCl and Cl₂ were within 15% when BrCl (0.1 to 1.3 ppb) was synthesized from the reaction of Br₂ (0.067 to 0.73 ppb) with excess Cl₂ (1.4 to 18.3 ppb). Changes in the instrument sensitivity, which were measured daily, have been taken into account.

19. B. J. Finlayson-Pitts, J. N. Pitts, *Chemistry of the Upper and Lower Atmosphere—Theory, Experiments, and Applications* (Academic Press, San Diego, CA, 2000).
20. J. F. Hopper, W. Hart, *J. Geophys. Res.* **99**, 25315 (1994).
21. U. K. Klänning, T. Wolff, *Ber. Bunsenges. Phys. Chem.* **89**, 243 (1985).
22. Some indirect light (twilight) is present at midday before 2 March, and even earlier further to the south, so the Br₂ and BrCl increases on day 60 to 61 could be photoinitiated.
23. K. W. Oum, M. J. Lakin, B. J. Finlayson-Pitts, *Geophys. Res. Lett.* **25**, 3923 (1998).
24. J. P. D. Abbatt, G. C. G. Waschewsky, *J. Phys. Chem. A* **102**, 3719 (1998).
25. R. Sander, P. J. Crutzen, *J. Geophys. Res.* **101**, 9121 (1996).
26. B. A. Michalowski et al., *J. Geophys. Res.* **105**, 15131 (2000).
27. T. X. Wang, D. W. Margerum, *Inorg. Chem.* **33**, 1050 (1994).
28. T. Koop, A. Kapilashrami, L. T. Molina, M. J. Molina, *J. Geophys. Res.* **105**, 26393 (2000).
29. S. Ghosal, A. Shbeeb, J. C. Hemminger, *Geophys. Res. Lett.* **27**, 1879 (2000).
30. E. M. Knipping et al., *Science* **288**, 301 (2000).
31. D. Toom-Sauntry, L. A. Barrie, *J. Geophys. Res.*, in press.
32. P. B. Shepson and D. Toom-Sauntry, unpublished data.
33. W. P. Bartlett, D. W. Margerum, *Environ. Sci. Technol.* **33**, 3410 (1999).
34. J. J. Orlando, B. Ramacher, G. Tyndall, *Geophys. Res. Lett.* **27**, 2633 (2000).
35. C. W. Spicer et al., *Nature* **394**, 353 (1998).
36. R. R. Dickerson et al., *J. Geophys. Res.* **104**, 21385 (1999).
37. C. W. Spicer, D. V. Kenny, W. J. Shaw, K. M. Busness, E. G. Chapman, *Environ. Sci. Technol.* **28**, 412A (1994).
38. We are grateful to the Department of Energy's Atmospheric Chemistry Program, and particularly P. Lunn, for support of this work; the Meteorological Service of Canada for providing transport to Alert and housing during the study; and the personnel of Canadian Forces Station Alert for logistical support. We are especially grateful for the on-site support provided by A. Gallant and P. Brickell, organizational support and comments on the manuscript by L. Barrie, use of a snow probe developed by A. L. Sumner, and ozone calibrations provided by K. Anlauf. We also thank J. N. Pitts Jr., J. C. Hemminger, P. Jungwirth, D. Tobias, and R. B. Gerber for helpful discussions and M. J. Molina for providing preprints before publication.

29 August 2000; accepted 6 December 2000

Widespread Origins of Domestic Horse Lineages

Carles Vilà,^{1*} Jennifer A. Leonard,² Anders Götherström,³ Stefan Marklund,⁴ Kaj Sandberg,⁴ Kerstin Lidén,³ Robert K. Wayne,² Hans Ellegren¹

Domestication entails control of wild species and is generally regarded as a complex process confined to a restricted area and culture. Previous DNA sequence analyses of several domestic species have suggested only a limited number of origination events. We analyzed mitochondrial DNA (mtDNA) control region sequences of 191 domestic horses and found a high diversity of matriline. Sequence analysis of equids from archaeological sites and late Pleistocene deposits showed that this diversity was not due to an accelerated mutation rate or an ancient domestication event. Consequently, high mtDNA sequence diversity of horses implies an unprecedented and widespread integration of matriline and an extensive utilization and taming of wild horses. However, genetic variation at nuclear markers is partitioned among horse breeds and may reflect sex-biased dispersal and breeding.

The domestication of the horse has profoundly affected the course of civilization. Horses provided meat, milk, and enhanced transportation and warfare capabilities that led to the spread of Indo-European languages and culture and the collapse of ancient societies (1, 2). Horse remains become increasingly common in archaeological sites of the Eurasian grassland steppe dating from about 6000 years ago, suggesting the time and place of their first domestication (3–5). Two alternative hypotheses for the origin of the domestic horse from wild populations can be formulated. A restricted origin hypothesis postulates that the domestic horse was developed through selective breeding of a limited

wild stock from a few foci of domestication. Thereafter, domestic horses would have been distributed to other regions. Under this hypothesis, domestication is a complex and improbable process requiring multigeneration selection on traits that permit stable coexistence with humans. Another alternative could be that domestication involved a large number of founders recruited over an extended time period from throughout the extensive Eurasian range of the horse. In this multiple origins scenario, horses may have been independently captured from diverse wild populations and then increasingly bred in captivity as wild numbers dwindled. Consequently, early domestic horses may not represent a stock highly modified by selective breeding.

These two hypotheses for the origin of the domestic horse make distinct predictions with regard to genetic variation in maternally inherited mtDNA. The restricted origin hypothesis predicts that mitochondrial diversity of the horse should be limited to a few founding lineages and those added subsequently by mutation. In contrast, a multiple origins hypothesis predicts diversity greater than that

typically found in a single wild population and divergence among lineages that well precedes the first evidence of domestication.

Phylogenetic analysis of 37 different mtDNA control region sequences from domestic horses deposited in GenBank, 616 base pairs (bp) in length (6), revealed at least six divergent sequence clades (clades A to F, Fig. 1A). After correcting for multiple hits and ignoring indels, the mean divergence observed between sequences was 2.6% (range: 0.2 to 5%). The average divergence between donkey (*Equus asinus*) and horses was 16.1% (range: 14.3 to 19.1%). Assuming that horses diverged from the lineage leading to extant stenoid equids (zebras and asses) at least 2 million years ago (Ma), as the fossil record suggests (7), or about 3.9 Ma, according to molecular data (8), we can estimate an average rate of equid mtDNA sequence divergence of 4.1% or 8.1% per million years. Therefore, modern horse lineages coalesce at about 0.32 or 0.63 Ma, long before the first domestic horses appear in the archaeological record (4). Even clade D, having a more recent coalescence time, has a mean sequence divergence of 0.8% (range: 0.2 to 2.0%), which predicts an origin at least 0.1 Ma. These results show that domestic horse lineages have an ancient origin. Thus, given the 6000-year origin suggested by the archaeological record, numerous matriline must have been incorporated into the gene pool of the domestic horse.

To expand the representation of modern and ancient breeds, we sequenced 355 bp of the left domain of the mtDNA control region in 191 horses from 10 distinct breeds (9), including some that are very old such as the Icelandic pony, Swedish Gotland Russ, and British Exmoor pony. A Przewalski's horse was also sequenced. We found 32 different sequences, and a search of GenBank provided 38 additional haplotypes for the same region. We compared all these sequences with those obtained from DNA isolated from long bone remains of eight horses preserved frozen in Alaskan permafrost deposits from a locality near Fairbanks, Alaska, dated 12,000 to 28,000 years ago (10, 11). Additionally, we sequenced DNA of eight

¹Department of Evolutionary Biology, Uppsala University, Norbyvägen 18D, S-75236 Uppsala, Sweden.

²Department of Organismic Biology, Ecology and Evolution, University of California, Los Angeles, CA 90095-1606, USA. ³Archaeological Research Laboratory, Stockholm University, S-10691 Stockholm, Sweden. ⁴Department of Animal Breeding and Genetics, Swedish University of Agricultural Sciences, S-75007 Uppsala, Sweden.

*To whom correspondence should be addressed. E-mail: carles.vila@ebc.uu.se